Industrial Crops & Products 139 (2019) 111517

Contents lists available at ScienceDirect

Industrial Crops & Products

journal homepage: www.elsevier.com/locate/indcrop

Galls of European *Fraxinus* trees as new and abundant sources of valuable phenylethanoid and coumarin glycosides

Moritz Zürn[a,b], Gergő Tóth[b,c], Márta Kraszni[c], Anna Sólyomváry[d], Zoltán Mucsi[e], Ruth Deme[f], Balázs Rózsa[g], Blanka Fodor[h], Ibolya Molnár-Perl[h], Kata Horváti[i], Szilvia Bősze[i], Bernadett Pályi[j], Zoltán Kis[j], Szabolcs Béni[d], Béla Noszál[c], Imre Boldizsár[a,b,*]

[a] Department of Plant Anatomy, Institute of Biology, Eötvös Loránd University, Pázmány Péter sétány 1/C, Budapest 1117, Hungary
[b] Eötvös Loránd University, Institutional Excellence Program, Natural Bioactive Compounds Group, Pázmány Péter sétány 1/C, Budapest 1117, Hungary
[c] Department of Pharmaceutical Chemistry, Semmelweis University, Hőgyes Endre u. 9, Budapest 1092, Hungary
[d] Department of Pharmacognosy, Semmelweis University, Üllői út 26, Budapest 1085, Hungary
[e] Femtonics Ltd., Tűzoltó u. 59, Budapest 1094, Hungary
[f] Department of Organic Chemistry, Semmelweis University, Hőgyes Endre u. 7, Budapest 1092, Hungary
[g] Institute of Experimental Medicine, Hungarian Academy of Sciences, Szigony u. 43, Budapest 1083, Hungary
[h] Department of Analytical Chemistry, Institute of Chemistry, Eötvös Loránd University, Pázmány Péter sétány 1/A, Budapest 1117, Hungary
[i] MTA-ELTE Research Group of Peptide Chemistry, Eötvös Loránd University, Hungarian Academy of Sciences, Budapest, Hungary
[j] National Public Health Center, Albert Flórián út 2-6, Budapest 1097, Hungary

ARTICLE INFO

Keywords:
Fraxinus
Acteoside
Cichoriin
Isomerization
Fragmentation
Vero cells

ABSTRACT

Irregular tissue outgrowths (called galls) in the inflorescences of three European *Fraxinus* species (*F. angustifolia*, *F. excelsior* and *F. ornus*), were analyzed for their phytochemical composition for the first time. The main goal of this study was to demonstrate the significance of *Fraxinus* galls as the new and abundant sources of drug candidate metabolites. The comparable quantitative results of nuclear magnetic resonance (NMR) spectroscopy and high performance liquid chromatography (HPLC)-mass spectrometry (MS) analyses confirmed extraordinarily high amounts of the valuable phenylethanoid glycoside (PhEG) acteoside (in the galls of *F. angustifolia* 86.7 mg/g – 139.9 mg/g and *F. excelsior* 71.7 mg/g – 161.2 mg/g) and that of the coumarin glucoside cichoriin (in the galls of *F. ornus* 143.0 mg/g – 232.0 mg/g). Optimized, consecutive treatments of acteoside, in distilled water (100 °C, 300 min) and acidic media (2 M trifluoroacetic acid, 100 °C, 15 min), resulted in an equilibrium of acteoside and isoacteoside as well as that of desrhamnosyl acteoside and desrhamnosyl isoacteoside, following isomerization and derhamnosylation, respectively. Three related PhEGs could thus also be isolated after optimized treatments, in addition to acteoside, in the highest yield reported so far. Their structures were identified by NMR spectroscopy and high-resolution Orbitrap-MS/MS techniques, also confirming the distinction of the regioisomers desrhamnosyl acteoside and desrhamnosyl isoacteoside by MS/MS. Molecular modeling was used to study the mechanism of isomerization. Isolated PhEGs and cichoriin showed no cytostatic activity in non-human primate Vero E6 cells and no hemolyis of human erythrocytes. Our results highlight the significance of *Fraxinus* galls in the production of PhEGs and cichoriin as easily available, high-yield harvestable, new raw materials for these pharmacologically important metabolites.

1. Introduction

Fraxinus angustifolia Vahl (narrow-leafed ash), *F. excelsior* L. (European ash) and *F. ornus* L. (flowering ash) are the three European representatives of the genus *Fraxinus*, belonging to the Oleaceae family. These deciduous trees are of great significance as ornamental, industrial and medicinal plants, and are cultivated in temperate regions worldwide (Wallander, 2008). The bark and the leaves of *F. excelsior* and *F. ornus* are recommended in European folk medicine, mainly against rheumatism and fever. The fruit extract of *F. ornus* is also used as an anti-diabetic agent. The dried leaf of *F. angustifolia* and *F. excelsior* has an official place in the European Pharmacopoeia (Ph.Eur. 9.2.) (Kostova, 2001; Kostova and Iossifova, 2007). The phytochemical composition of *Fraxinus*' organs, including bark, leaf, inflorescence and

* Corresponding author at: Department of Plant Anatomy, Institute of Biology, Eötvös Loránd University, Pázmány Péter sétány 1/C, Budapest 1117, Hungary.
E-mail address: boldizsarimi@gmail.com (I. Boldizsár).

https://doi.org/10.1016/j.indcrop.2019.111517
Received 27 February 2019; Received in revised form 25 June 2019; Accepted 26 June 2019
Available online 01 July 2019

fruit, has been extensively studied. In fact, caffeoylquinic acids, coumarins, phenylethanoid glycosides (PhEGs) and secoiridoids have been identified as the most valuable secondary metabolites of these trees (Kostova, 2001; Kostova and Iossifova, 2007).

The inflorescences of *Fraxinus* trees frequently contain abnormal outgrowths of plant tissues, known as galls. These galls can be caused by the phytophagous mite *Aceria fraxinivorus*, which attacks the inflorescences, resulting in sizable, irregular deformities formed mainly from the flower stalks (Ripka and De Lillo, 1997). High-yield harvesting of galls from infected *Fraxinus* trees is feasible, without damaging the plants (Supplementary material, Figs. S1, S2). As the characteristic metabolites of the European *Fraxinus* species are present in all the organs investigated so far, we hypothesized the accumulation of these metabolites in the gall tissues also. The galls of the *Fraxinus* species might thus be a novel, abundant source of valuable secondary metabolites; however, to the best of our knowledge, there is no published data about their phytochemical composition. Our preliminary analyses of these galls suggested a high-level accumulation of the PhEG acteoside (AO) and that of the coumarin glucoside cichoriin.

Acteoside (syn. verbascoside) is constructed from a centrally positioned β-*D*-glucose that is connected via glycosidic bonds to hydroxytyrosol and α-*L*-rhamnose units, as well as via an ester bond to a caffeic acid molecule at the C1 − OH, C3 − OH and C4 − OH positions, respectively (Fig. 1). Acteoside was already identified in different organs of European *Fraxinus* species (Lamaison et al., 1993). In addition to *Fraxinus* trees, more than 200 plant species contain AO (Alipieva et al., 2014). A regioisomer of AO, the isoacteoside (IsAO, syn. isoverbascoside), which is esterified with caffeic acid at the C6 − OH position (Fig. 1), and the corresponding desrhamnosyl derivatives of AO and IsAO, desrhamnosyl AO (DeAO, syn. calceolarioside A) and desrhamnosyl IsAO (DeIsAO, syn. calceolarioside B), are also present in some AO containing plants as minor compounds. The rarely occurring coumarin glucoside cichoriin (Fig. 1) is known in some plants belonging to the Asteraceae and Oleaceae families (Kostova, 2001).

These PhEGs and the coumarin glucoside cichoriin may be promising medicinal agents, as all four PhEGs have significant antioxidant (Harput et al., 2012; Bardakci et al., 2015; Li et al., 2018), antiproliferative (Nagao et al., 2001; Harput et al., 2012) and antiviral (Kernan et al., 1998; Kim et al., 2002; Brandão et al., 2013) effects. AO and IsAO also exhibited neuroprotective (Li et al., 2018), anti-inflammatory (Díaz et al., 2004) immune-enhancing (Huang et al., 2009) and xanthine oxidase inhibitory (Chen et al., 2018) activities and cichoriin expressed hepatoprotective (Xu et al., 2016) and antibacterial (El-Bassuony and Abdel-Hamid, 2006) effects.

Prior to performing further efficacy studies with these PhEGs and cichoriin, their *in vitro* cytotoxic side effects on mammalian cells, such as the hemolytic activity on human erythrocytes and cytostatic activity on Vero E6 cell line, should also be investigated. Vero E6 cells are kidney epithelial cells isolated from *Cercopithecus aethiops* and often used in microbiology as a host cell model for a class of intracellular pathogens (such as slow growing viruses and bacteria). In this model, promising drug candidates should have no cytotoxic or cytostatic effect against the Vero E6 cells and no hemolytic effect against human red blood cells, as we have previously reported (Horváti et al., 2017). Recently, AO alone was tested for its cytotoxicity against Vero E6 cells among four PhEGs and cichoriin, and its non-toxicity in the concentration range applied (0–200 μg/mL) was confirmed (Brandão et al., 2013).

The isomerization of AO into IsAO (Mazzutti et al., 2017) and the derhamnosylation of AO and IsAO (Nagao et al., 2001) during heat treatments performed in water and acidic media, respectively, and the mass fragmentation patterns of AO, IsAO, DeAO and DeIsAO, were also described (Keefover-Ring et al., 2014; Tóth et al., 2014; Chen et al., 2018), however the regioisomer pairs AO - IsAO and DeAO - DeIsAO were not distinguished from each other by their specific fragment ions. Conversion procedures (isomerization and hydrolysis) were not optimized regarding yields (avoiding unwanted decompositions) and time consumption.

The aim of this research was to 1) determine the main secondary plant metabolites in the galls of the three European *Fraxinus* species (*F. angustifolia*, *F. excelsior* and *F. ornus*), 2) confirm the high-level accumulation of AO and cichoriin using comparative techniques, *i.e.*, HPLC-MS and quantitative nuclear magnetic resonance (qNMR) spectroscopy, 3) optimize the heat treatments of AO in water and acidic media, in order to obtain IsAO, DeAO and DeIsAO at the highest yield possible, allowing the isolation of all four related compounds by one-step preparative HPLC, 4) interpret the isomerization process at the atomic level using a computational method, 5) analyze MS fragment profiles in order to determine diagnostic ions suitable for the distinction of regioisomers AO and IsAO as well as DeAO and DeIsAO, 6) determine the *in vitro* toxicity (against Vero E6 cells) and the hemolytic activity (in human erythrocytes) of AO, IsAO, DeAO, DeIsAO and cichoriin, 7) evaluate the real potential of *Fraxinus* galls for the high-yield isolation of PhEGs.

2. Materials and methods

2.1. Plant material and reagents

Gall samples of *Fraxinus angustifolia* Vahl, *F. excelsior* L. and *F. ornus* L. were collected from different Hungarian locations in July and August 2015. These galls were caused by the phytophagous mite *Aceria fraxinivorus* (Ripka and De Lillo, 1997).

The voucher specimens (FrAng-2015-01–05, FrExc-2015-01-05 and FrOrn-2015-01-05) were deposited in the Department of Plant Anatomy, Eötvös Loránd University, Budapest, Hungary. The materials and reagents applied in the isolation and analysis of gall metabolites, such as acetonitrile (ACN), distilled water (DW), formic acid, methanol (Reanal, Hungary), methanol-d_4 (99.80% D), deuterium oxide (D_2O -99.96% D) (VWR chemicals, Belgium), dimethyl sulfoxide (DMSO), maleic acid standard for qNMR, 3-(trimethylsilyl)-1-propanesulfonic acid-d_6 sodium salt (DSS-d_6), aesculin, chlorogenic acid (Sigma-Aldrich, USA) and trifluoroacetic acid (TFA; Serva, Germany) were all of analytical reagent grade of the highest purity available.

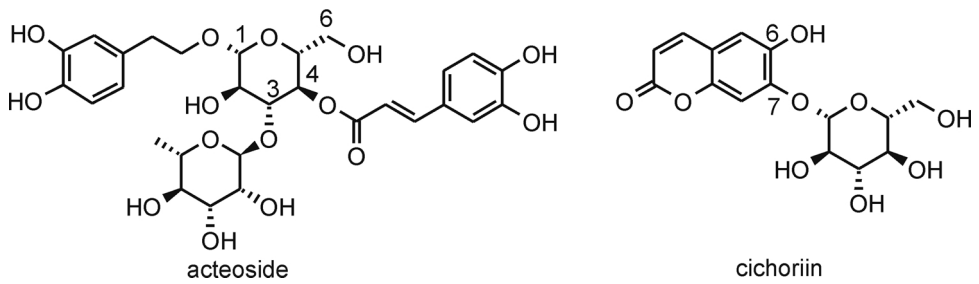

Fig. 1. Chemical structures of acteoside and cichoriin.

2.2. Preparation of gall extracts

Lyophilized and pulverized gall samples (100.0 mg) were extracted three times consecutively with 5 mL of methanol at 60 °C, via a reflux condenser, for 30 min, to prepare 15.0 mL stock solutions. These stock solutions were used after their dilution with methanol for HPLC-UV-HR-MS analyses (Section 2.4.1.). Dried aliquots (5.0 mL) of the stock solution prepared from *F. angustifolia* gall sample 1 and *F. ornus* gall sample 3, were dissolved in 1.0 mL of methanol (for the isolation of AO and cichoriin by preparative HPLC, Section 2.4.2), DW (for performing heat treatments, Section 2.3.2.) and methanol-d_4 (for performing NMR analyses (Section 2.4.3).

2.3. Performing heat treatments in DW and TFA media

2.3.1. Treatment optimization of isolated acteoside

0.624 mg amounts of isolated AO were dissolved in 1.0 mL DW, 0.2 M TFA, 0.6 M TFA and 2 M TFA (in 4 mL screw-capped vials). These solutions were heated for 7, 15, 30, 60, 120, 300 and 600 min at either 50 °C or 100 °C. The samples were dried using a vacuum evaporator (at 30–40 °C). The dried samples were analyzed after their dissolution in methanol by HPLC-UV-HR-MS (Section 2.4.1.).

2.3.2. Optimized treatments of gall extracts for isolation purposes

Dried aliquots (5.0 mL) of the stock solution prepared from *F. angustifolia* gall sample 1, were dissolved in 1.0 mL DW to isolate IsAO, DeAO and DeIsAO. This solution was heated at 100 °C for 300 min (as optimum condition) to prepare the IsAO. A two-step heating procedure was applied to prepare the DeAO and DeIsAO. The first step was the same as that for IsAO preparation, and then TFA (0.181 mL) was added to the DW solution to prepare 2 M TFA medium. In the second step of treatment, this acidified solution was heated at 100 °C for 15 min (as optimum condition). After heat treatment, the samples were dried using a vacuum evaporator (at 30–40 °C). The dried samples were dissolved in methanol before isolations performed using preparative HPLC (Section 2.4.2.).

2.4. Instruments

2.4.1. Analytical HPLC hyphenated with UV and high-resolution Orbitrap mass spectrometric detections

A Dionex Ultimate 3000 UHPLC system (3000RS diode array detector (DAD), TCC-3000RS column thermostat, HPG-3400RS pump, SRD-3400 solvent rack degasser, WPS-3000TRS autosampler), hyphenated with a Orbitrap Q Exactive Focus Mass Spectrometer equipped with electrospray ionization (ESI) (Thermo Fischer Scientific, Waltham, MA, USA) was used for chromatographic separation and high resolution mass spectral analysis. The HPLC separations were performed on a Kinetex C18 column (75 × 3.0 mm; 3.5 µm) (Phenomenex, USA). The mobile phase consisted of 0.1% v/v formic acid (A) and acetonitrile (B). Linear gradient: 0.0 min, 20% B; 12.0 min, 60% B; flow rate: 0.3 mL/min; column temperature: 25 °C; injected volume: 1.0 µL. The ESI source was operated in negative ionization mode and operation parameters were optimized automatically using the built-in software. The working parameters were as follows: spray voltage, 2500 V (-); capillary temperature 320 °C; sheath-, auxiliary- and spare-gases (N_2): 47.52, 11.25 and 2.25 arbitrary units, respectively. The resolution of the full scan was of 70,000 and the scanning range was between 100–1000 *m/z* units. MS/MS scans were acquired at a resolution of 35,000 in the range of 80–1000 *m/z* units, using collision energy of 10, 20, 30 and 45 eV. DAD spectra were recorded between 250 and 600 nm.

2.4.2. Preparative HPLC

A Pharmacia LKB HPLC (Uppsala, Sweden) system (2248 pumps, VWM 2141 UV detector) was connected to a preparative HPLC column: Nucleosil100, C18 (10 µm), 15 × 1 cm (Teknokroma, Sant Cugat del Vallès, Barcelona, Spain). The eluents, gradient program and detection were the same as described above, except for the flow rate and injected amount, which were 3.0 mL/min and 200 µL, respectively.

2.4.3. Nuclear magnetic resonance (NMR) spectroscopy

NMR spectra of the isolated compounds were recorded in methanol-d_4 at 25 °C on a Varian DDR spectrometer (599.9 MHz for ^{1}H and 150.9 MHz for ^{13}C) equipped with a dual 5 mm inverse detection gradient (IDPFG) probe-head.

For the qNMR experiments, three parallel dried gall extracts of *F. ornus* (sample 3) and *F. angustifolia* (sample 1) were dissolved in 1.0 ml methanol-d_4 and 530 µL of these solutions were transferred into 5 mm NMR tubes. Approximately 5 mM of DSS-d_6 solution, prepared in D_2O, was placed in a coaxial insert tube and used as external reference. The apparent, precise concentration of the DSS-d_6 peak was determined as the average of three additional NMR measurements using maleic acid standard solutions prepared in methanol-d_4 in three different concentrations (NMR methods are detailed in the Supplementary material).

2.5. Compound quantification by HPLC-MS

In order to quantify compounds by HPLC-MS, extracted ion chromatograms (EICs) of their molecular ions were recovered from the total ion current chromatograms, and an external standard method was applied by using EICs. Linear regression analysis of the isolated AO, IsAO, DeAO and DeIsAO, as well as that of the standard aesculin and chlorogenic acid, was performed in the range of 0.057–10.0 ng of their injected amounts, resulting in appropriate r^2 values (Supplementary material Table S1). Amounts of cichoriin and methoxy-dihydroxycoumarin-glucoside were calculated using the calibration curve for standard aesculin.

2.6. Computational method

All computations were carried out with the Gaussian09 program package (Gaussian Inc., USA, Wallingford CT, 2009) (Frisch et al., 2016) using standard convergence criteria of 3.0×10^{-4}, 4.5×10^{-4}, 1.2×10^{-3} and 1.8×10^{-3}, for the gradients of the root mean square (RMS) force, maximum force, RMS displacement, and maximum displacement vectors, respectively. Computations were carried out at the B3LYP level of theory (Becke, 1993) using /6–31 G(d,p) basis set. The explicit-implicit solvent model was also included using the IEFPCM method (radii = UFF) (Tomasi et al., 2005) and seven explicit water molecules to model the aqueous media properly (Mucsi et al., 2005). The vibrational frequencies were computed at the same levels of theory, in order to properly confirm all structures as residing at the minima on their potential energy hypersurfaces (PESs). The thermodynamic functions U, H, G and S were computed at 298.15 K.

2.7. In vitro activity of PhEGs and coumarins on non-human primate Vero cell cultures and human erythrocytes

The cytostatic effect of isolated PhEGs, cichoriin and standard aesculin was measured on Vero E6 cells (non-human primate origin; *Cercopithecus aethiops*, kidney, epithelial cells; ATCC No. CRL-1586) (Emeny and Morgan, 1979). The Vero E6 cells were kindly provided by Bernadett Pályi (National Biosafety Laboratory, National Public Health Institute, Hungary). Cells were maintained in DMEM (Lonza™) as described earlier (Palyi et al., 2018). Prior to treatment, cells were plated (5000 cells, 100 µl/well) in a flat-bottom 96-well plate. Stock solutions of the compounds were prepared with DMSO (50 mM) and two-fold serial dilution series were prepared using serum free DMEM (final concentration: 0.8–100 µM). Cells were incubated with the compounds for 24 h. Control cells were treated with serum free medium only, or with DMSO containing serum free medium (cDMSO = 0.1% v/v) at 37 °C. A membrane-active cationic peptide (Transportan) was used as a

cytostatic positive control (Horváti et al., 2017). After incubation, cells were washed twice with serum free medium (centrifugation: 1000 rpm, 5 min). To determine the *in vitro* cytostatic effects, the cells were cultured for a further 72 h in serum containing medium. The cell viability was determined using the classic endpoint assay (4,5-dimethylthiazol-2-yl)-2,5-diphenyltetrazolium bromide (MTT)-assay described by Mossman (Mosmann, 1983) and modified (Horváti et al., 2017). In each case two independent experiments were carried out with four parallel measurements. The 50% inhibitory concentration (IC_{50}) values were determined from the dose-response curves.

4 v/v % red blood cell (RBC) suspensions were prepared for hemolytic activity assay (Horváti et al., 2017). Stock solutions of the compounds were diluted with DMSO (50 mM) and two-fold serial dilution series were prepared (final concentration: 0.8–100 µM). RBC suspensions (100 µl/well, 4 v/v %) were placed into a 96-well U-bottom cell culture plate and mixed with 100 µl solutions of compounds. The plates were incubated for 1.5 h at 37 °C. After centrifugation (2000 rpm, 5 min), 50 µl of the supernatant was transferred to a flat-bottom microtiter plate and absorbance was measured at λ = 414 and 450 nm using the ELISA plate reader. A cationic membrane active peptide (CM15) was used as hemolytic positive control (Horváti et al., 2017). The percentage hemolysis was graphically presented and the concentration of compound at which 50% hemolysis occurred (HC_{50} value) was determined.

3. Results and discussion

3.1. Identification of gall compounds

The HPLC-UV-HR-MS separations of *F. angustifolia*, *F. excelsior* and *F. ornus* gall extracts show similar metabolite compositions (Fig. 2). Based on HR-MS data, compounds appearing with comparable retentions in the chromatograms of gall extracts of the three species are identified by identical molecular formulas (Table 1). Comparing this data with that obtained for already identified compounds of *Fraxinus* species, a coumarin glucoside (Fa-1, Fe-1, Fo-1) and its methoxy derivative (Fa-3, Fe-3, Fo-3), four PhEGs that differ from each other by the presence (Fa-5, Fa-7, Fe-5, Fe-7, Fo-5, Fo-7) or absence (Fa-4, Fa-6, Fe-4, Fe-6, Fo-4, Fo-6) of a rhamnosyl moiety, as well as an isomer of caffeoylquinic acid (Fa-2 and Fe-2), were presumed to be present in *F. angustifolia* (Fa-1 – Fa-7), *F. excelsior* (Fe-1 – Fe-7) and *F. ornus* (Fo-1 – Fo-7) gall extracts (Fig. 2).

Since these compounds may all be present as regioisomers, further analyses, (*i.e.*, NMR, HPLC-HR-MS/MS as well as conversion studies) were conducted in order to determine their constitutions. Accordingly, the NMR spectral data of whole methanol extract of *F. ornus* gall confirmed the identity of the main compound Fo-1 as cichoriin (7-*O*-glucoside of dihydroxycoumarin, Fig. 1) (Supplementary material Fig. S3) (Kisiel and Michalska, 2002).

Unlike *F. ornus* gall, the galls of the other two *Fraxinus* species contained only a minor compound (Fa-1 and Fe-1, Fig. 2, Table 1), which can be identified using the molecular formula $C_{15}H_{16}O_9$ and a retention time identical with that of cichoriin, however the UV spectral data of cichoriin (Fo-1) and Fa-1/Fe-1, demonstrating characteristic differences in their wavelengths of absorption maxima (λ_{max}, Fo-1: 288 nm, 340 nm; Fa-1 and Fe-1: 293 nm, 334 nm), confirmed Fa-1 and Fe-1 to be the 6-*O*-glucoside of dihydroxycoumarin, as aesculin (Fig. 1) (Harborne, 1984). Methoxy-dihydroxycoumarin-glucosides Fa-3, Fe-3 and Fo-3 were also identified by HPLC-HR-MS, although without confirming their conformation.

The mass spectra of the molecular ion of the caffeoylquinic acid isomer (*m/z* 353; Fa-2, Fe-2), obtained by HPLC-HR-MS/MS, exhibited a base peak at *m/z* 191.06 and two low intensity peaks (< 5%, relative to the base peak) at *m/z* 179.03 and *m/z* 135.04. This result is consistent with recent experience (Clifford et al., 2005), confirming the presence of 5-caffeoylquinic acid (chlorogenic acid) in *F. angustifolia* and *F. excelsior* galls. As a further confirmation, standard chlorogenic acid was also analyzed by HPLC-HR-MS/MS, resulting in comparable mass fragmentation and retention properties to those for compounds Fa-2 and Fe-2.

The PhEG Fa-5, identified as the main compound in *F. angustifolia* gall, was isolated using preparative HPLC for its precise identification. Solutions of Fa-5 prepared in DW or TFA, were heated at 100 °C for different periods of time and analyzed by HPLC-HR-MS/MS (Figs. 3 and 4). In fact, the heating of Fa-5 in DW and TFA resulted in the formation of compounds appearing with longer (Fa-7, Fig. 3C, DW treated sample) and shorter retentions (Fa-4, Fig. 3D, TFA treated sample) relative to Fa-5, respectively. The molecular formula of Fa-7 was determined as $C_{29}H_{36}O_{15}$, based on HPLC-HR-MS results, which was the same as that of Fa-5 (Table 1). The chromatographic and mass spectral data for Fa-5 and Fa-7 was comparable to that reported in the literature for AO and IsAO, respectively, thereby confirming the identity of Fa-5 and Fa-7 as

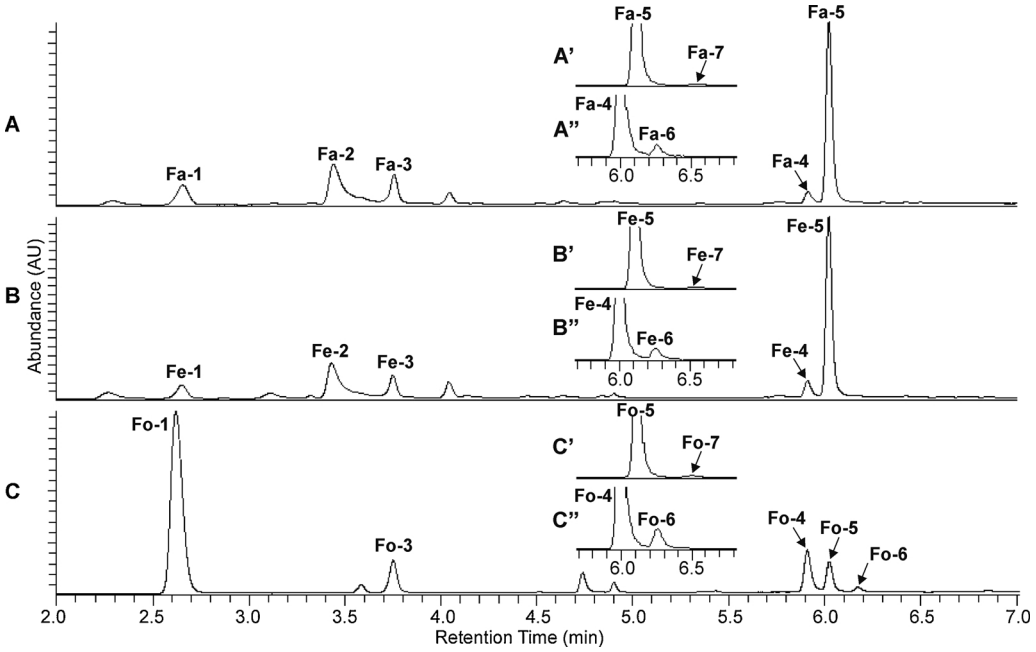

Fig. 2. HPLC separation of the extracts prepared from *F. angustifolia* gall sample 1 (A, A', A''), *F. excelsior* gall sample 1 (B, B', B'') and *F. ornus* gall sample 1 (C, C', C''). Full chromatograms (A, B, C) were recorded using UV detection (λ280 nm), and trace chromatograms (A', A'', B', B'', C', C'') were obtained by MS detection, monitoring the extracted ion current for *m/z* 623 (A', B', C') and *m/z* 477 (A'', B'', C'') corresponding to phenylethanoid glycosides. Peaks: Fa-1, Fe-1 aesculin; Fo-1 cichoriin; Fa-2, Fe-2 chlorogenic acid; Fa-3, Fe-3, Fo-3 methoxy-dihydroxycoumarin-glucoside; Fa-4, Fe-4, Fo-4 desrhamnosyl acteoside; Fa-5, Fe-5, Fo-5 acteoside; Fa-6, Fe-6, Fo-6 desrhamnosyl isoacteoside; Fa-7, Fe-7, Fo-7 isoacteoside.

Table 1
High resolution mass-spectral (negative ion mode) data for compounds detected in *F. angustifolia* (Fa-1 – Fa-7), *F. excelsior* (Fe-1 – Fe-7) and *F. ornus* (Fo-1 – Fo-7) gall extracts.

Ret. time	Gall sample			Formula	Detected formula	Detected ion	Calculated *m/z*	Found *m/z*	diff (ppm)
	F. ang.[c] Compounds	*F. exc.*[d]	*F. ornus*						
2.66[a]	Fa-1			$C_{15}H_{16}O_9$	$[M-H]^-$	$C_{15}H_{15}O_9$	339.07106	339.07233	3.750
2.65[a]		Fe-1						339.07221	3.396
2.62[a]			Fo-1					339.07233	3.750
3.44[a]	Fa-2			$C_{16}H_{18}O_9$	$[M-H]^-$	$C_{16}H_{17}O_9$	353.08671	353.08817	4.139
3.43[a]		Fe-2						353.08795	3.516
–			–					–	–
3.76[a]	Fa-3			$C_{16}H_{18}O_{10}$	$[M-H]^-$	$C_{16}H_{17}O_{10}$	369.08162	369.08301	3.758
3.75[a]		Fe-3						369.08279	3.162
3.75[a]			Fo-3					369.08298	3.676
6.00[b]	Fa-4			$C_{23}H_{26}O_{11}$	$[M-H]^-$	$C_{23}H_{25}O_{11}$	477.13914	477.14038	2.603
5.99[b]		Fe-4						477.14043	2.708
5.99[b]			Fo-4					477.14047	2.792
6.10[b]	Fa-5			$C_{29}H_{36}O_{15}$	$[M-H]^-$	$C_{29}H_{35}O_{15}$	623.19705	623.19879	2.797
6.10[b]		Fe-5						623.19863	2.541
6.10[b]			Fo-5					623.19861	2.509
6.25[b]	Fa-6			$C_{23}H_{26}O_{11}$	$[M-H]^-$	$C_{23}H_{25}O_{11}$	477.13914	477.14026	2.353
6.25[b]		Fe-6						477.14036	2.561
6.25[b]			Fo-6					477.14031	2.456
6.50[b]	Fa-7			$C_{29}H_{36}O_{15}$	$[M-H]^-$	$C_{29}H_{35}O_{15}$	623.19705	623.19850	2.332
6.50[b]		Fe-7						623.19838	2.140
6.51[b]			Fo-7					623.19852	2.364

[a] HPLC-UV.
[b] HPLC-MS retention times (min) of compounds correspond to those in Fig. 2.
[c] *F. angustifolia*.
[d] *F. excelsior*.

these PhEG type regioisomers. As further confirmations, i) computational calculations interpreting the isomerization of AO into IsAO at atomic level, (Section 3.2), and ii) NMR analysis of whole methanol extract of *F. angustifolia* gall sample, confirming the identity of AO (Supplementary material Fig. S4), were also performed.

The difference between the molecular formulas of AO (Fa-5, Table 1) and Fa-4 (Table 1) is consistent with the loss of a rhamnosyl moiety ($C_6H_{10}O_4$), and thus the formation of Fa-4 from AO during TFA treatment can be explained by the hydrolysis of glycosidic bond between rhamnose and glucose units of AO, forming the corresponding desrhamnosyl derivate of AO. A DW treated sample containing comparable amounts of AO and IsAO (Fig. 3C), was also heated in TFA medium, resulting in the derhamnosylation of both compounds. DeAO and DeIsAO were thus equally detected (Fig. 3E).

Starting with a sample containing AO, the other three related PhEGs, IsAO, DeAO and DeIsAO, can also be prepared by consecutive DW and TFA treatments, however treatment conditions, temperature, time and acid concentration, need to be optimized in order to minimize unwanted decomposition. Acteoside treatment processes were therefore performed using DW and different concentrations of TFA (0.2 M, 0.6 M and 2 M) at 50 °C and 100 °C, applying various heating times from 7 min to 600 min. To demonstrate the conversion characteristics of compounds on a comparable basis, their amounts are given in mM values as shown in Fig. 4A–D.

At 50 °C, AO remained intact, and its conversion products could not be identified either in DW or in TFA treated samples. However, at 100 °C, characteristic conversions occurred as a result of simultaneous isomerization, derhamnosylation and undefined degradation processes (Fig. 4A–D). The isomerization of AO into IsAO was detected in DW at 100 °C, accompanied by negligible derhamnosylation and significant undesired degradation of AO and IsAO. The highest IsAO yield was determined after heating for 300 min (0.35 mM, Fig. 4A). Comparing the ratios of IsAO and AO amounts between samples heated in DW at 100 °C for different periods of time, a maximum value of 1.2 was

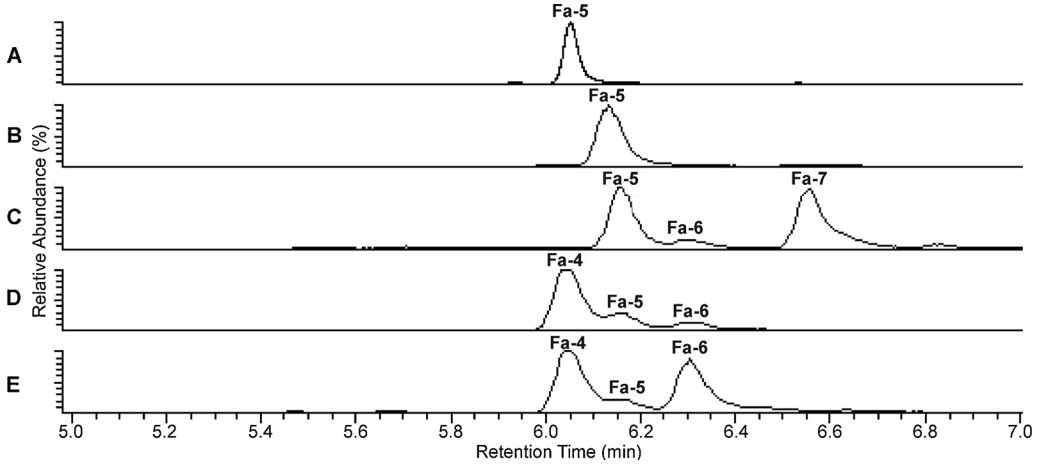

Fig. 3. HPLC-UV (λ280 nm) chromatogram (A) and extracted ion chromatograms (B – E) for *m/z* 623 + *m/z* 477 corresponding to phenylethanoid glycosides (PhEGs), obtained from the intact acteoside sample (A, B), and from the acteoside sample after distilled water - DW (C, 100 °C, 120 min) and trifluoroacetic acid - TFA (D, 100 °C, 15 min) treatments, as well as from the acteoside sample after consecutive treatments performed in DW (100 °C, 120 min) and 2 M TFA (100 °C, 15 min) media (E).

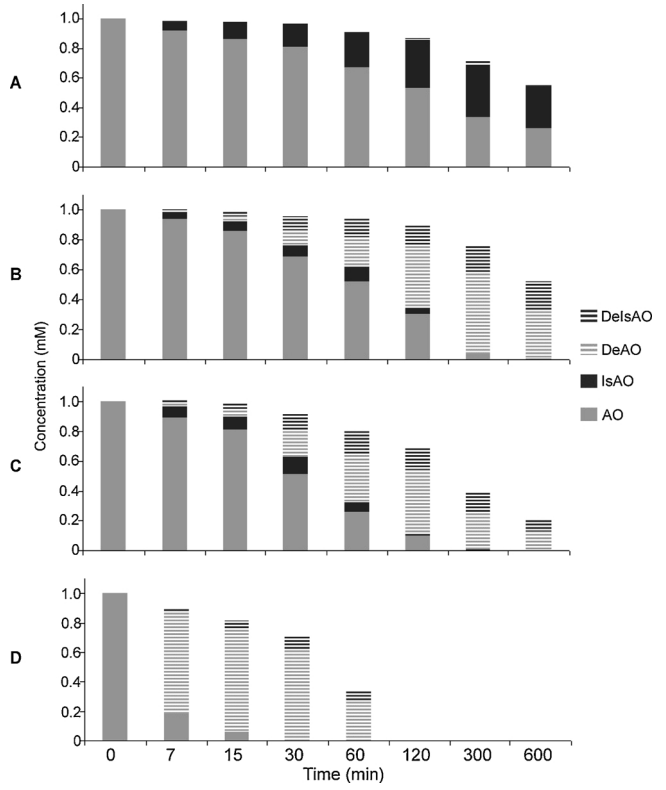

Fig. 4. Comparison of the composition of phenylethanoid glycosides in isolated acteoside samples that were heated at 100 °C with distilled water - DW (A), 0.2 M trifluoroacetic acid - TFA (B), 0.6 M TFA (C) and 2 M TFA (D), for different periods of time (from 0 min to 600 min). Corresponding chromatograms of samples treated with DW for 120 min and 2 M TFA for 15 min, are shown in Fig. 3C and D, respectively.

calculated after heating for 600 min (0.31 mM/0.26 mM = 1.2; Fig. 4A). This result is in good accordance with data obtained using the computational method (as detailed in Section 3.2.), indicating that IsAO is slightly more stable in DW than AO.

In addition to isomerization and undesired degradation, the acid treatment at 100 °C led to intense derhamnosylation, resulting in the formation of DeAO as a main product. Its highest yield was determined in a 2 M TFA solution heated for 15 min (0.70 mM, Fig. 4D). Similarly, when AO and IsAO were equally present (as the result of DW heating at 100 °C for 300 min), their 2 M TFA treatment (100 °C, 15 min) resulted in the formation of comparable amounts of DeAO and DeIsAO, as shown in Fig. 3E. The following optimum treatment conditions were thus applied for the preparative isolation of selected PhEGs: i) DW heating (100 °C, 300 min) for IsAO, and ii) consecutive heating in DW (100 °C, 300 min) and 2 M TFA (100 °C, 15 min) for DeAO and DeIsAO isolation.

Additional NMR spectral data for AO, IsAO, DeAO and DeIsAO, isolated from their optimum sources, was comparable to that reported in the literature for these PhEGs, thereby unambiguously confirming their identity (Schlauer et al., 2004; Oh et al., 2005). In accordance with the literature (Keefover-Ring et al., 2014; Chen et al., 2018), identical fragment ions were observed for the regioisomer pairs AO - IsAO and DeAO - DeIsAO (Table 2), however based on our results, the difference in the relative ion intensities of two key fragment ions *m/z* 179 and *m/z* 315, corresponding to the deprotonated caffeic acid and hydroxytyrosol glucoside moieties, allowed the discrimination of DeAO and DeIsAO. Analyzing the fragment ion spectra generated from the molecular ions of DeAO and DeIsAO using a collision induced dissociation (CID, 30 eV), calculated ion abundance ratios *m/z* 179/315 as 8.0 and 0.27 for DeAO and DeIsAO, respectively (average results,

Table 2
Relative intensities of selective fragment ions, generated from the molecular ions of phenylethanoid glycosides (PhEGs) by collision induced dissociation (CID, 30 eV), followed by HPLC-high-resolution Orbitrap-MS/MS analyses of three injected amounts of PhEGs.

Phenylethanoid glycosides	Injected amounts (ng)	Selective fragment ions (SFIs), *m/z*				
		135	161	179	315	461
		Relative intensities (%)[a]				
acteoside	10.0	4.7	67.0	1.4	1.8	6.9
	5.0	4.7	67.3	2.0	1.5	7.2
	1.0	6.1	69.2	1.2	1.4	7.7
isoacteoside	10.0	4.5	57.6	2.2	1.5	11.5
	5.0	4.2	58.2	2.0	1.9	11.1
	1.0	6.5	57.6	1.7	2.0	10.7
desrhamnosyl acteoside	6.4	5.0	63.2	12.6	1.5	–
	3.2	5.0	61.9	11.9	1.5	–
	0.64	5.1	71.0	14.0	1.9	–
desrhamnosyl isoacteoside	5.7	4.6	66.2	1.6	6.3	–
	2.85	4.0	71.6	1.6	6.5	–
	0.57	4.9	70.9	2.3	7.2	–

[a] Expressed as percentages of the total product ion current (Full MS2).

calculated from the relative ion intensities of three different injected amounts of DeAO and DeIsAO) (Table 2).

3.2. Computational modeling of the isomerization of AO into IsAO

The isomerization of AO into IsAO is an intramolecular acyl transfer reaction (Mucsi et al., 2005, 2008a, 2008b; Kovács et al., 2018), where the caffeoyl ester moiety of AO migrates from the C4 − OH position to the neighboring C6-hydroxyl group, resulting in the formation of IsAO (Fig. 1, Supplementary material Fig. S5). The thermodynamic (driving force) and kinetic (reaction rate) aspects of this transformation were both studied using theoretical methods at the B3LYP/6–31 G(d,p) (Becke, 1993) level of theory, with the IEFPCM solvent model (Tomasi et al., 2005) by Gaussian 09 (Frisch et al., 2016).

From a thermodynamic point of view, the transformation is slightly exothermic, as the enthalpy (ΔH) and Gibbs free energy (ΔG) decrease equally by -1.0 kJ mol^{-1} and -2.8 kJ mol^{-1}, respectively (Supplementary material Fig. S5). These values suggest an equilibrium process with an equilibrium constant (K) of 0.4 between AO and IsAO. As we confirmed previously, acyl transfer reactions can also be characterized by the change of the carbonylicity percentage (CA%) value (Mucsi et al., 2008a, 2008b; Kovács et al., 2018). In fact, the increase of this value means a beneficial process. The calculated CA% values of AO and IsAO proved to be comparable, 52.8% and 53.0%, respectively, confirming the absence of the internal driving force for the transformation, as was also confirmed by the enthalpy (ΔH) change. The overall cause of the transformation thus comes from the beneficial entropy change (ΔS, + 6.0 J mol^{-1} K^{-1}) derived from the sterically less hindered and more freely rotating side-chain.

The reaction mechanism was also studied to estimate the reaction rate of the isomerisation, using an explicit-implicit solvent model (Supplementary material Fig. S6, Tables S2, S3) (Mucsi et al., 2005). According to this model, isomerization consisting of two elementary steps allows a relatively fast reaction rate.

3.3. Amounts of compounds found in the galls of *F. angustifolia*, *F. excelsior* and *F. ornus*

The quantitative HPLC-MS analyses of 15 gall samples collected from five different habitats of *F. angustifolia, F. excelsior and F. ornus*, showed extraordinarily high amounts of AO (86.7–139.9 mg/g and 71.7–161.2 mg/g in galls of *F. angustifolia* and *F. excelsior*, respectively) and cichoriin (143.0–232.0 mg/g in galls of *F. ornus*) (Table 3). To confirm these remarkable results, triplicate parallels of methanol

Table 3
Composition of the dried gall samples of three *Fraxinus* species, determined by HPLC-MS.

Fraxinus species	Gall samples (GSs)[a]	Amounts of compounds in the dried gall samples (mg/g)[b]						
		Aesculin or cichoriin[c]	CA	MeDCG	AO	IsAO	DeAO	DeIsAO
F. angustifolia	GS-1	14.2	38.6	13.5	128.0	1.06	8.09	0.556
	GS-2	6.05	30.1	8.52	101.3	2.25	3.34	0.482
	GS-3	13.3	30.6	11.3	112.4	0.985	4.63	0.494
	GS-4	10.3	24.9	7.18	86.7	0.706	4.82	0.400
	GS-5	18.0	41.0	15.5	139.9	1.86	8.08	0.822
	average	12.4	33.0	11.2	113.7	1.37	5.79	0.551
F. excelsior	GS-1	12.1	39.8	15.2	161.2	1.73	15.0	1.15
	GS-2	17.9	24.8	18.8	122.5	0.996	21.3	1.04
	GS-3	10.8	18.3	9.50	88.7	0.887	20.7	2.01
	GS-4	4.65	6.43	15.9	71.7	2.79	15.6	4.95
	GS-5	16.0	24.2	16.3	132.1	0.991	15.0	1.01
	average	12.3	22.7	15.1	115.2	1.48	17.5	2.03
F. ornus	GS-1	165.3	–	20.2	20.1	0.396	25.7	3.85
	GS-2	143.0	–	33.3	13.5	0.569	17.4	5.85
	GS-3	193.2	–	11.2	9.29	0.311	28.0	3.17
	GS-4	232.0	–	13.1	24.8	0.204	7.93	0.996
	GS-5	170.7	–	10.1	8.59	0.374	31.2	2.99
	average	180.8	–	17.6	15.3	0.371	22.0	3.37

CA: chlorogenic acid, MeDCG: methoxy-dihydroxycoumarin-glucoside, AO: acteoside, IsAO: isoacteoside, DeAO: desrhamnosyl acteoside, DeIsAO: desrhamnosyl isoacteoside.

[a] GSs 1–5 were collected from different localities of *Fraxinus* trees.

[b] Values are the averages of three separate extractions. Differences could be characterized by the relative standard deviation (RSD) values, ranging from 2.38% (AO in *F. angustifolia* GS-1) to 4.78% (CA in *F. excelsior* GS-2).

[c] GSs of *F. angustifolia* and *F. excelsior* contain aesculin and GSs of *F. ornus* contain cichoriin.

extracts of *F. angustifolia* (sample 1) and those of *F. ornus* (sample 3) galls were also analyzed using quantitative HPLC-MS and qNMR spectroscopy. The differences were characterized by the relative standard deviation percentages (RSD%) of the three parallel tests: i) 128.0 mg/g (2.38 RSD%) and 119.3 mg/g (2.96 RSD%) AO in *F. angustifolia* (gall sample 1); and ii) 193.2 mg/g (3.02 RSD%) and 185.8 mg/g (2.24 RSD %) cichoriin in *F. ornus* (gall sample 3) were determined using HPLC-MS and qNMR analyses, respectively. Based on these comparable results (128.0 *vs*. 119.3 mg/g AO and 193.2 *vs*. 185.8 mg/g cichoriin) obtained using the two different quantitation methods (HPLC-MS and qNMR), the high-yield accumulation of AO and cichoriin in *Fraxinus* galls was clearly confirmed.

Based on literature review, AO is a minor compound in many species, but its abundant sources were also determined, such as the dried leaves of *Sesamum indicum* (129 mg/g) and *Ligustrum purpurascens* (13–73 mg/g) (Li et al., 2012; Fuji et al., 2018,). Our research group also recently determined high levels of AO in the different organs of *Euphrasia rostkoviana* (25.6 mg/g), *Syringa vulgaris* (24.8 mg/g) and *Olea europaea* (17.2 mg/g) (Tóth et al., 2014, 2015, 2016). However, the highest amount of AO, which could be isolated from 100 mg plant material (dried leaves of *Stachys sieboldii*), was only 2.5 mg (corresponds to 2.5% isolated yield of AO) (Nishimura et al., 1991). The average AO contents in the galls of *F. angustifolia* (113.7 mg/g) and *F. excelsior* (115.2 mg/g) (Table 3) correspond to those reported as the highest in the plant kingdom, and the average cichoriin content in galls of *F. ornus* (180.8 mg/g) is six times higher than its highest amount found to date (30 mg/g, *F. ornus* flower) (Kostova, 2001), thus highlighting the significance of *Fraxinus* galls in the production of these valuable metabolites.

The conventional taxonomic classification of *F. angustifolia*, *F. excelsior* and *F. ornus* trees (Wallander, 2008) showed close correlations with the phytochemical composition of their galls: i) the high-level accumulation of AO and the absence of cichoriin in the two representatives of the section *Fraxinus* (*F. angustifolia*, *F. excelsior*), and ii) the presence of cichoriin in *F. ornus* belonging to section *Ornus*, were found to be characteristic.

3.4. Practical utility of Fraxinus galls in the isolation of PhEGs

F. angustifolia gall sample 1 was used in order to isolate PhEGs, as its AO content (124.0 mg/g, average of HPLC-MS and NMR quantitations) represents a mean value among *F. angustifolia* and *F. excelsior* galls (Table 3). Accordingly, 12.4 mg AO could be isolated as the theoretical maximum yield (TMY) from methanol extract of 100.0 mg gall sample 1. The isolation procedure could be regarded to be effective, according to a comparison of the TMY of AO (12.4 mg) with the amount of AO isolated by preparative HPLC from 100.0 mg sample 1 (8.5 mg), resulting in the highest isolated yield of AO (8.5%) among plants, thus confirming the significance of *Fraxinus* galls in AO production.

Starting from the 100.0 mg sample 1: i) 4.7 mg IsAO after optimized DW treatment (100 °C, 300 min), and ii) 0.97 mg DeAO and 1.3 mg DeIsAO after consecutive, optimized DW (100 °C, 300 min) and TFA (2 M TFA, 100 °C, 15 min) treatments, were isolated. A review of the content of these three PhEGs among plants found that 37.3 mg/g of IsAO (Gómez-Aguirre et al., 2012), 0.8 mg/g of DeAO (Taskova et al., 2005) and 2.5 mg/g of DeIsAO (Jensen, 1996) were the highest amounts, in *Castilleja tenuiflora* (dried root culture), *Isoplexis sceptrum* (fresh leaf) and *Nematanthus wettsteinii* (fresh plant), respectively. The amounts of IsAO, DeAO and DeIsAO isolated from *F. angustifolia* galls, were 1.3, 12.1 and 5.2 times higher than those reported as the highest for these compounds in the plant kingdom to date.

An evaluation of the harvestable gall yield is also needed to confirm the practical significance of *Fraxinus* galls in the large-scale production of these valuable metabolites. Since gall production is the result of a mite infection, the occurrence of galls is not guaranteed on all *Fraxinus* trees, however if this frequently occurring infection is present, extraordinarily high numbers of galls may be collected, without harming the host plant itself. In fact, the maximum yields harvested, from $\approx 1\ m^3$ crown of *F. angustifolia*, *F. excelsior* and *F. ornus*, 0.6 kg, 0.9 kg and 0.4 kg galls, respectively, suggest the potential for the industrial-scale isolation of PhEGs and that of cichoriin.

3.5. In vitro activity of isolated PhEGs (AO, IsAO, DeAO and DeIsAO) and cichoriin as well as standard aesculin on non-human primate Vero E6 cell culture and on human erythrocytes

In vitro profiling of four PhEGs and two coumarins started with the assay on Vero E6 cells and human red blood cells (erythrocytes). No cytostatic activity occurred on Vero E6 cells after treatment with all PhEGs and coumarins in the concentration range of 0.8–100 μM. A cationic membrane active peptide (Transportan) was applied as a positive control, which demonstrated relevant cytostatic activity on the Vero E6 culture (IC_{50} = 33.9 ± 5.5μM), (Supplementary material Fig S7). This is the first report of the non-cytostatic activity of IsAO, DeAO, DeIsAO, aesculin and cichoriin on this cell type.

The hemolytic activity of PhEGs and coumarins was tested on freshly prepared human red blood cells as described earlier (Horváti et al., 2017). The PhEGs and coumarins showed no hemolytic activity in the tested concentration range (0.8–100 μM). In contrast, the cationic membrane-active peptide (CM15), which was used as positive control in this study, was hemolytic at HC_{50} = 45.2 ± 2.3 μM concentration (Supplementary material Fig S7). According to our results, further *in vitro* efficacy tests against intracellular pathogens can be carried out with all these PhEGs and coumarins, using Vero E6 cells as the host cell model.

4. Conclusions

Analysis of the gall composition of the three European *Fraxinus* species confirmed an extraordinarily high amount of the valuable phenylethanoid glycoside AO (in the galls of *F. angustifolia* and *F. excelsior*) and of the coumarin cichoriin (in the galls of *F. ornus*). Optimized, consecutive DW and TFA treatments of AO resulted in its isomerization, forming an equilibrium of AO and IsAO and the derhamnosylation of AO and IsAO into DeAO and DeIsAO thus, allowing the high-yield isolation of these four PhEGs. HPLC-HR Orbitrap-MS/MS fragmentation studies of isolated PhEGs confirmed that the regioisomers DeAO and DeIsAO are distinguished based on the ion intensities of two key fragment ions *m/z* 179 and *m/z* 315. PhEGs (AO, IsAO, DeAO and DeIsAO) and coumarins (aesculin and cichoriin) showed no cytostatic activity on Vero E6 cells and no hemolytic activity on human red blood cells; therefore further *in vitro* profiling on different systems (such as against intracellular pathogens) can be carried out for all these compounds. Our results highlight the significance of *Fraxinus* galls in the production of PhEGs and cichoriin as easily available, high-yield harvestable, new raw materials of these valuable metabolites.

Acknowledgements

This work was supported by the National Research, Development and Innovation Office, Hungary (grants: VEKOP-2.3.3-15-2017-00020, VEKOP-2.3.2-16-2017-00014, OTKA 115431, OTKA 124077, KFI_16-1-2016-0177, NVKP_16-1-2016-0043), by the János Bolyai Research Scholarship of the Hungarian Academy of Sciences (to I. Boldizsár, S. Béni, K. Horváti and G. Tóth), by the Bolyai + New National Excellence Program (grant number: ÚNKP-18-4-SE-121) of the Ministry of Human Capacities (S. Béni) and by the Semmelweis Innovation Found STIA-M-17 and STIA-18-KF (to G. Tóth). This work was completed in the ELTE Institutional Excellence Program (1783-3/2018/FEKUTSRAT) supported by the Hungarian Ministry of Human Capacities.

Appendix A. Supplementary data

Supplementary material related to this article can be found, in the online version, at doi:https://doi.org/10.1016/j.indcrop.2019.111517.

References

Alipieva, K., Korkina, L., Orhan, I.E., Georgiev, M.I., 2014. Verbascoside - a review of its occurrence, (bio)synthesis and pharmacological significance. Biotechnol. Adv. 32, 1065–1076. https://doi.org/10.1016/j.biotechadv.2014.07.001.

Bardakci, H., Skaltsa, H., Milosevic-Ifantis, T., Lazari, D., Hadjipavlou-Litina, D., Yeşilada, E., Kırmızıbekmez, H., 2015. Antioxidant activities of several *Scutellaria* taxa and bioactive phytoconstituents from *Scutellaria hastifolia* L. Ind. J. Crop. Prod. Process. 77, 196–203. https://doi.org/10.1016/j.indcrop.2015.08.027.

Becke, A.D., 1993. Density-functional thermochemistry. III. The role of exact exchange. J. Chem. Phys. 98, 5648–5652. https://doi.org/10.1063/1.464913.

Brandão, G.C., Kroon, E.G., Souza, D.E., Souza Filho, J.D., Oliveira, A.B., 2013. Chemistry and antiviral activity of *Arrabidaea pulchra* (Bignoniaceae). Molecules 18, 9919–9932. https://doi.org/10.3390/molecules18089919.

Chen, X., Deng, Z., Huang, X., Geng, C., Chen, J., 2018. Liquid chromatography–mass spectrometry combined with xanthine oxidase inhibition profiling for identifying the bioactive constituents from *Cistanche deserticola*. Int. J. Mass Spectrom. 430, 1–7. https://doi.org/10.1016/j.ijms.2018.03.009.

Clifford, M.N., Knight, S., Kuhnert, N., 2005. Discriminating between the six isomers of dicaffeoylquinic acid by LC-MS(n). J. Agric. Food Chem. 53, 3821–3832. https://doi.org/10.1021/jf050046h.

Díaz, A.M., Abad, M.J., Fernandez, L., Silván, A.M., De Santos, J., Bermejo, P., 2004. Phenylpropanoid glycosides from *Scrophularia scorodonia*: in vitro anti-inflammatory activity. Life Sci. 74, 2515–2526. https://doi.org/10.1016/j.lfs.2003.10.008.

El-Bassuony, A.A., Abdel-Hamid, N., 2006. Antibacterial coumarins isolated from *Launaea resedifolia*. Химия растительного сырья. 1, 65–68.

Emeny, J.M., Morgan, M.J., 1979. Regulation of the interferon system: evidence that Vero cells have a genetic defect in interferon production. J. Gen. Virol. 43, 247–252. https://doi.org/10.1099/0022-1317-43-1-247.

Frisch, M.J., Trucks, G.W., Schlegel, H.B., Scuseria, G.E., Robb, M.A., Cheeseman, J.R., et al., 2016. Gaussian 16 Rev. B.01. CT, Wallingford.

Fuji, Y., Uchida, A., Fukahori, K., Chino, M., Ohtsuki, T., Matsufuji, H., 2018. Chemical characterization and biological activity in young sesame leaves (*Sesamum indicum* L.) and changes in iridoid and polyphenol content at different growth stages. PLoS One 13. https://doi.org/10.1371/journal.pone.0194449.

Gómez-Aguirre, Y.A., Zamilpa, A., González-Cortazar, M., Trejo-Tapia, G., 2012. Adventitious root cultures of *Castilleja tenuiflora* Benth. As a source of phenylethanoid glycosides. Ind. Crop. Prod. 36, 188–195. https://doi.org/10.1016/j.indcrop.2011.09.005.

Harborne, J.B., 1984. Methods of Plant Analysis, Phytochemical Methods. Springer, Dordrecht, pp. 1–36.

Harput, U.S., Genc, Y., Saracoglu, I., 2012. Cytotoxic and antioxidative activities of *Plantago lagopus* L. and characterization of its bioactive compounds. Food Chem. Toxicol. 50, 1554–1559. https://doi.org/10.1016/j.fct.2012.01.019.

Horváti, K., Bacsa, B., Mlinkó, T., Szabo, N., Hudecz, F., Zsila, F., Bősze, S., 2017. Comparative analysis of internalisation, haemolytic, cytotoxic and antibacterial effect of membrane-active cationic peptides: aspects of experimental setup. Amino Acids 49, 1053–1067. https://doi.org/10.1007/s00726-017-2402-9.

Huang, D.F., Tang, Y.F., Nie, S.P., Wan, Y., Xie, M.Y., Xie, X.M., 2009. Effect of phenylethanoid glycosides and polysaccharides from the seed of *Plantago asiatica* L. On the maturation of murine bone marrow-derived dendritic cells. Eur. J. Pharmacol. 620, 105–111. https://doi.org/10.1016/j.ejphar.2009.07.025.

Jensen, S.R., 1996. Caffeoyl phenylethanoid glycosides in *Sanango racemosum* and in the Gesneriaceae. Phytochemistry 43, 777–783. https://doi.org/10.1016/0031-9422(96)00186-0.

Keefover-Ring, K., Holeski, L.M., Bowers, M.D., Clauss, A.D., Lindroth, R.L., 2014. Phenylpropanoid glycosides of *Mimulus guttatus* (yellow monkeyflower). Phytochem. Lett. 10, 132–139. https://doi.org/10.1016/j.phytol.2014.08.016.

Kernan, M.R., Amarquaye, A., Chen, J.L., Chan, J., Sesin, D.F., Parkinson, N., Ye, Z., Barrett, M., Bales, C., Stoddart, C.A., Sloan, B., Blanc, P., Limbach, C., Mrisho, S., Rozhon, E.J., 1998. Antiviral phenylpropanoid glycosides from the medicinal plant *Markhamia lutea*. J. Nat. Prod. 61, 564–570. https://doi.org/10.1021/np9703914.

Kim, H.J., Yu, Y.G., Park, H., Lee, Y.S., 2002. HIV gp41 binding phenolic components from *Fraxinus sieboldiana* var. Angustata. Planta Med. 68, 1034–1036. https://doi.org/10.1055/s-2002-35665.

Kisiel, W., Michalska, K., 2002. A new coumarin glucoside ester from *Cichorium intybus*. Fitoterapia 73, 544–546. https://doi.org/10.1016/S0367-326X(02)00172-7.

Kostova, I., 2001. *Fraxinus ornus* L. Fitoterapia 72, 471–480. https://doi.org/10.1016/S0367-326X(00)00340-3.

Kostova, I., Iossifova, T., 2007. Chemical components of *Fraxinus* species. Fitoterapia 78, 85–106. https://doi.org/10.1016/j.fitote.2006.08.002.

Kovács, E., Rózsa, B., Csomos, A., Csizmadia, I.G., Mucsi, Z., 2018. Amide activation in ground and excited states. Molecules 23. https://doi.org/10.3390/molecules23112859.

Lamaison, J., Petit Jean-Freytet, C., Carnat, A., 1993. Verbascoside, major phenolic compound of ash leaves (*Fraxinus excelsior*) and Vervain (*Aloysia triphylla*). Plant Med. Phytother. 26, 225–233.

Li, L., Xu, L.J., Peng, Y., He, Z.D., Shi, R.B., Xiao, P.G., 2012. Simultaneous determination of five phenylethanoid glycosides in small-leaved Kudingcha from the *Ligustrum* genus by UPLC/PDA. Food Chem. 131, 1583–1588. https://doi.org/10.1016/j.foodchem.2011.10.018.

Li, M., Xu, T., Zhou, F., Wang, M., Song, H., Xiao, X., Lu, B., 2018. Neuroprotective effects of four phenylethanoid glycosides on H(2)O(2)-induced apoptosis on PC12 cells via the Nrf2/ARE pathway. Int. J. Mol. Sci. 19, 1135. https://doi.org/10.3390/ijms19041135.

Mazzutti, S., Ferreira, S.R.S., Herrero, M., Ibañez, E., 2017. Intensified aqueous-based processes to obtain bioactive extracts from Plantago major and *Plantago lanceolata*. J. Supercrit. Fluids 119, 64–71. https://doi.org/10.1016/j.supflu.2016.09.008.

Mosmann, T., 1983. Rapid colorimetric assay for cellular growth and survival: application to proliferation and cytotoxicity assays. J. Immunol. Methods 65, 55–63. https://doi.org/10.1016/0022-1759(83)90303-4.

Mucsi, Z., Chass, G.A., Csizmadia, I.G., 2008a. Amidicity change as a significant driving force and thermodynamic selection rule of transamidation reactions. A synergy between experiment and theory. J. Phys. Chem. B 112, 7885–7893. https://doi.org/10.1021/jp8023292.

Mucsi, Z., Chass, G.A., Viskolcz, B., Csizmadia, I.G., 2008b. Quantitative scale for the extent of conjugation of carbonyl groups: "carbonylicity" percentage as a chemical driving force. J. Phys. Chem. A 112, 9153–9165. https://doi.org/10.1021/jp8048586.

Mucsi, Z., Szabó, A., Hermecz, I., Kucsman, A., Csizmadia, I.G., 2005. Modeling rate-controlling solvent effects. The pericyclic meisenheimer rearrangement of N-propargylmorpholine N-oxide. J. Am. Chem. Soc. 127, 7615–7631. https://doi.org/10.1021/ja042227q.

Nagao, T., Abe, F., Okabe, H., 2001. Antiproliferative constituents in the plants 7. Leaves of *Clerodendron bungei* and leaves and bark of *C. Trichotomum*. Biol. Pharm. Bull. 24, 1338–1341. https://doi.org/10.1248/bpb.24.1338.

Nishimura, H., Sasaki, H., Inagaki, N., Chin, M., Mitsuhashi, H., 1991. Nine phenethyl alcohol glycosides from *Stachys sieboldii*. Phytochemistry 30, 965–969. https://doi.org/10.1016/0031-9422(91)85288-B.

Oh, J.W., Lee, J.Y., Han, S.H., Moon, Y.H., Kim, Y.G., Woo, E.R., Kang, K.W., 2005. Effects of phenylethanoid glycosides from *Digitalis purpurea* L. on the expression of inducible nitric oxide synthase. J. Pharm. Pharmacol. 57, 903–910. https://doi.org/10.1211/0022357056451.

Palyi, B., Magyar, N., Henczko, J., Szalai, B., Farkas, A., Strecker, T., Takacs, M., Kis, Z., 2018. Determining the effect of different environmental conditions on Ebola virus viability in clinically relevant specimens. Emerg. Microbes Infect. 7, 52. https://doi.org/10.1038/s41426-018-0043-z.

Ripka, G., De Lillo, E., 1997. New data to the knowledge on the eriophyoid fauna in Hungary (Acari: eriophyoidea). Folia ent. hung. 58, 147–158.

Schlauer, J., Budzianowski, J., Kukulczanka, K., Ratajczak, L., 2004. Acteoside and related phenylethanoid glycosides in *Byblis liniflora* Salisb. Plants propagated in vitro and its systematic significance. Acta Soc. Bot. Pol. 73, 9–15. https://doi.org/10.5586/asbp.2004.002.

Taskova, R.M., Gotfredsen, C.H., Jensen, S.R., 2005. Chemotaxonomic markers in Digitalideae (Plantaginaceae). Phytochemistry 66, 1440–1447. https://doi.org/10.1016/j.phytochem.2005.04.020.

Tomasi, J., Mennucci, B., Cammi, R., 2005. Quantum mechanical continuum solvation models. Chem. Rev. 105, 2999–3093. https://doi.org/10.1021/cr9904009.

Tóth, G., Alberti, Á., Sólyomváry, A., Barabás, C., Boldizsár, I., Noszál, B., 2015. Phenolic profiling of various olive bark-types and leaves: HPLC–ESI/MS study. Ind. Crop. Prod. 67, 432–438. https://doi.org/10.1016/j.indcrop.2015.01.077.

Tóth, G., Barabás, C., Tóth, A., Kéry, Á., Béni, S., Boldizsár, I., Varga, E., Noszál, B., 2016. Characterization of antioxidant phenolics in *Syringa vulgaris* L. Flowers and fruits by HPLC-DAD-ESI-MS. Biomed. Chromatogr. 30, 923–932. https://doi.org/10.1002/bmc.3630.

Tóth, G., Sólyomváry, A., Boldizsár, I., Noszál, B., 2014. Characterization of enzyme-catalysed endogenous β-hydroxylation of phenylethanoid glycosides in *Euphrasia rostkoviana* Hayne at the molecular level. Process Biochem. 49, 1533–1537. https://doi.org/10.1016/j.procbio.2014.05.023.

Wallander, E., 2008. Systematics of *Fraxinus* (Oleaceae) and evolution of dioecy. Plant Sys. Evol. 273, 25–49. https://doi.org/10.1007/s00606-008-0005-3.

Xu, K., Feng, Z.-M., Yang, Y.-N., Jiang, J.-S., Zhang, P.-C., 2016. Eight new eudesmane- and eremophilane-type sesquiterpenoids from *Atractylodes lancea*. Fitoterapia. 114, 115–121. https://doi.org/10.1016/j.fitote.2016.08.017.